

Interaction-induced transition in the quantum chaotic dynamics of a disordered metal

S.V. Syzranov,^{1,2} A.V. Gorshkov,^{2,3} and V.M. Galitski^{2,4}

¹*Physics Department, University of California, Santa Cruz, CA 95064, USA*

²*Joint Quantum Institute, NIST/University of Maryland, College Park, MD 20742, USA*

³*Joint Center for Quantum Information and Computer Science,
NIST/University of Maryland, College Park, MD 20742, USA*

⁴*Condensed Matter Theory Center, Physics Department,
University of Maryland, College Park, MD 20742, USA*

(Dated: June 16, 2022)

We demonstrate that a weakly disordered metal with short-range interactions exhibits a transition in the quantum chaotic dynamics when changing the temperature or the interaction strength. For weak interactions, the system displays exponential growth of the out-of-time-ordered correlator (OTOC) of the current operator. The Lyapunov exponent of this growth is temperature-independent in the limit of vanishing interaction. With increasing the temperature or the interaction strength, the system undergoes a transition to a non-chaotic behaviour, for which the exponential growth of the OTOC is absent. We conjecture that the transition manifests itself in the quasiparticle energy-level statistics and also discuss ways of its explicit observation in cold-atom setups.

A classical chaotic system is a system whose evolution is exponentially sensitive to the initial conditions. Because small perturbations of the Hamiltonian or the initial state of a chaotic system may dramatically change its dynamics, its evolution may appear random even without any random elements in the Hamiltonian.

The concept of chaos in *quantum* systems is more subtle and has several different widely used definitions. When a quantum system has a well-defined classical limit, this system is often called chaotic if the classical limit of its dynamics is chaotic. Another definition of quantum chaos involves energy-level statistics. When the dynamics of a system is apparently random, one may expect this system to be described by the random-matrix theory, which leads to the Wigner-Dyson statistics of the energy levels. An immense amount of numerical data (see Ref. [1] for review) suggests that various systems with Wigner-Dyson level statistics, such as disordered metals and non-integrable billiards, exhibit classical chaotic dynamics, thereby confirming the equivalence of the two definitions in these cases.

Numerous recent studies suggest another notion of quantum chaos, which is related to the exponential growth of out-of-time-ordered correlators (OTOCs) of Hermitian operators, quantities of the form $\langle [\hat{A}(t), \hat{B}(0)]^2 \rangle$. Such correlators were first introduced half a century ago [2] for electrons in weakly disordered metals; it was demonstrated that the correlator of the single-momentum projections grows exponentially, $\langle [\hat{p}_z(t), \hat{p}_z(0)]^2 \rangle \propto \exp(2\lambda t)$, where the exponent λ gives the rate of divergence between two initially close classical electron trajectories. However, exponential growth of OTOCs in quantum systems takes place only on sufficiently short times, in contrast with classical chaotic dynamics.

The last couple of years have seen an upsurge of research activity (see, for example, Refs. [3–22]) on OTOCs

and quantum chaos, in part motivated by a recent prediction [3] of the bound $\lambda \leq 2\pi T/\hbar$ on the Lyapunov exponent in strongly interacting systems at temperature T . OTOCs are also expected [5–8, 10] to distinguish between many-body-localised [23][24] and many-body-delocalised phases. Despite recent advances in rigorous microscopic calculations of OTOCs in disordered interacting systems (see, e.g., Refs. [4, 10–12]), the generic conditions for the existence of chaotic behaviour in such systems still remain to be investigated.

In this paper, we demonstrate that weakly disordered interacting systems exhibit a phase transition from quantum-chaotic to non-chaotic behaviour when increasing the temperature or the interaction strength. We distinguish between chaotic and non-chaotic behaviour via the OTOC of momentum projections.

Results. We demonstrate that in a weakly disordered system with short-range interactions, the time dependence of the OTOC of momentum \hat{P}_z of the entire system is given by

$$F(t) = \langle [\hat{P}_z(t), \hat{P}_z(0)]^2 \rangle \propto \exp \left[2\lambda t - \frac{2t}{\tau(T)} \right], \quad (1)$$

where we omitted the subleading terms, which at $t = 0$ ensure the vanishing of the correlator; the averaging $\langle \dots \rangle$ is carried out with respect to both the state of the electrons and disorder realisations; T is the temperature; λ is the classical Lyapunov exponent in a non-interacting disordered system; and $1/\tau(T) \propto T^2$ is the rate of inelastic quasiparticle scattering at the Fermi surface. Depending on which term in the exponent dominates, the OTOC exhibits exponential growth or lack thereof.

At low temperatures and interaction strengths, the behaviour of the system is similar to that in the absence of interactions, with an exponentially growing OTOC, which comes from pairs of close electron trajectories and from energies in the interval $\varepsilon \sim T$ near

the Fermi surface. The Lyapunov exponent λ is determined by the quasiparticle parameters at the Fermi surface and is temperature-independent, in contrast with strongly-interacting systems, where a temperature-dependent bound on the Lyapunov exponent was conjectured [3]. The exponential growth only persists for t shorter than the Ehrenfest time $t_E = \lambda^{-1} \ln(ap_F)$ (hereinafter $\hbar = 1$), where a is the characteristic impurity size and p_F is the Fermi momentum.

For large temperatures and strong interactions, inelastic large-momentum scattering destroys correlations between electrons with close trajectories and thus suppresses the exponential growth. There exists a critical temperature (or interaction strength, for a given temperature) which corresponds to $\tau(T) = \lambda^{-1}$ and separates the regimes of exponential growth and the lack of exponential growth. We conjecture that the transition from chaotic to non-chaotic behaviour is accompanied by a change of quasiparticle energy-level statistics from Wigner-Dyson to Poisson or to other types of statistics. The transition may also be observed explicitly in double layers of ultracold atoms or molecules exposed to a random potential.

Model. We consider a weakly disordered metal in dimension $d > 1$ described by the Hamiltonian

$$\hat{\mathcal{H}} = \int \hat{\Psi}^\dagger(\mathbf{r}) \left[\xi_{\mathbf{k}} + \sum_i U(\mathbf{r} - \mathbf{r}_i) \right] \hat{\Psi}(\mathbf{r}) d\mathbf{r} + \int \hat{\Psi}^\dagger(\mathbf{r}) \hat{\Psi}^\dagger(\mathbf{r}') w(\mathbf{r} - \mathbf{r}') \hat{\Psi}(\mathbf{r}') \hat{\Psi}(\mathbf{r}) d\mathbf{r} d\mathbf{r}', \quad (2)$$

where $\hat{\Psi}^\dagger$ and $\hat{\Psi}$ are fermionic operators, $\xi_{\mathbf{k}}$ is the operator of the kinetic energy; there are identical randomly located impurities in the system, with $U(\mathbf{r} - \mathbf{r}_i)$ being the potential of the i -th impurity; $w(\mathbf{r} - \mathbf{r}')$ is the interaction potential between two particles, which is assumed to be short-range in this paper. Here we disregard the spin degree of freedom, because it has no qualitative effect on our results.

Formalism. Describing transport in a disordered system often involves perturbative expansions in interactions and random potential, using Wick's theorem to reduce observables in various orders of perturbation theory to two-point correlators, i.e. Green's functions [25]. A similar approach may be adopted when calculating four-point OTOCs [4], defining Green's functions on a four-branch time contour instead of the conventional two-branch Keldysh contour [26].

Here we use an alternative approach, developed recently in Ref. [27], which consists in deriving kinetic (or master) equations for higher-order correlators, similar to the joint distribution functions of two copies of the sys-

tem of electrons. We introduce four correlation functions

$$K^{\alpha\beta}(\mathbf{r}_1, \mathbf{r}_{1'}; \mathbf{r}_2, \mathbf{r}_{2'}; t) = \left\langle \left[\hat{\Psi}^{\alpha\dagger}(\mathbf{r}_1, t) \hat{\Psi}^\alpha(\mathbf{r}_{1'}, t), \hat{P}_z(0) \right] \left[\hat{\Psi}^{\beta\dagger}(\mathbf{r}_2, t) \hat{\Psi}^\beta(\mathbf{r}_{2'}, t), \hat{P}_z(0) \right] \right\rangle, \quad (3)$$

where each of the indices α and β may take two values: e (electron) or h (hole); $\hat{\Psi}^\alpha(\mathbf{r}) = \hat{\Psi}(\mathbf{r})$ is the annihilation operator for an electron at location \mathbf{r} and $\hat{\Psi}^h = \hat{\Psi}^\dagger(\mathbf{r})$ is the hole annihilation operator. The time evolution of the correlators K^{ee} , K^{hh} and $K^{eh,he}$ is similar to the evolution of the joint distribution functions of two electrons, two holes and electron-hole pairs, respectively. Moreover, for a system in a classical environment, of which a random potential is a special case, the evolution of the correlators (3) exactly matches that of the density matrix of pairs of electrons and/or holes, respectively [27].

The relation of the OTOC of momentum projections to the correlation functions $K^{\alpha\beta}$ is given by

$$F(t) = \int_{\mathbf{R}_1, \mathbf{R}_2, \mathbf{p}_1, \mathbf{p}_2} p_{1z} p_{2z} K^{ee}(\mathbf{p}_1, \mathbf{R}_1; \mathbf{p}_2, \mathbf{R}_2; t), \quad (4)$$

where our conventions for coordinate and momentum integration are $\int_{\mathbf{R}} \dots = \int \dots d\mathbf{R}$ and $\int_{\mathbf{p}} \dots = \int \dots \frac{d\mathbf{p}}{(2\pi)^d}$, respectively, in the d -dimensional space; $K^{ee}(\mathbf{p}_1, \mathbf{R}_1; \mathbf{p}_2, \mathbf{R}_2; t)$ is the Wigner-transform (a function of the centre-of-mass coordinates $\mathbf{R}_i = \frac{\mathbf{r}_i + \mathbf{r}_{i'}}{2}$ and the Fourier-transform of the coordinate difference, $\mathbf{r}_i - \mathbf{r}_{i'} \rightarrow \mathbf{p}_i$) of the correlation function $K^{ee}(\mathbf{r}_1, \mathbf{r}_{1'}; \mathbf{r}_2, \mathbf{r}_{2'}; t)$. Equation (4) is similar to the relation between the correlator $\langle p_{1z} p_{2z} \rangle$ of the momentum projections of two electrons and the joint density matrix of these electrons.

The initial values of the correlators (3) for an electron gas with the (single-particle) distribution function $f_{\mathbf{k}}$ are given by

$$K^{\alpha\alpha}(\mathbf{p}_1, \mathbf{R}_1; \mathbf{p}_2, \mathbf{R}_2; 0) = -K^{\alpha\bar{\alpha}}(\mathbf{p}_1, \mathbf{R}_1; \mathbf{p}_2, \mathbf{R}_2; 0) = \partial_{Z_1} \partial_{Z_2} g(\mathbf{R}_1 - \mathbf{R}_2, \mathbf{p}_1 - \mathbf{p}_2), \quad (5)$$

where $\bar{\alpha}$ labels an ‘‘antiparticle’’ of α ($\bar{e} = h$; $\bar{h} = e$); ∂_{Z_1} and ∂_{Z_2} are derivatives with respect to the z components of \mathbf{R}_1 and \mathbf{R}_2 ; the function $g(\mathbf{R}_1 - \mathbf{R}_2, \mathbf{p}_1 - \mathbf{p}_2)$ is given by

$$g(\mathbf{R}_1 - \mathbf{R}_2, \mathbf{p}_1, \mathbf{p}_2) = -(4\pi)^d \delta(\mathbf{p}_1 - \mathbf{p}_2) \int_{\mathbf{q}} f_{\mathbf{p}_1 - \mathbf{q}} (1 - f_{\mathbf{p}_1 + \mathbf{q}}) e^{2i\mathbf{q} \cdot (\mathbf{R}_1 - \mathbf{R}_2)} \quad (6)$$

and is sharply peaked at the origin as a function of $\mathbf{R}_1 - \mathbf{R}_2$ and $\mathbf{p}_1 - \mathbf{p}_2$.

Impurity scattering. In a non-interacting system, electron wavepackets move along classical trajectories at sufficiently short times. When two classical electrons with

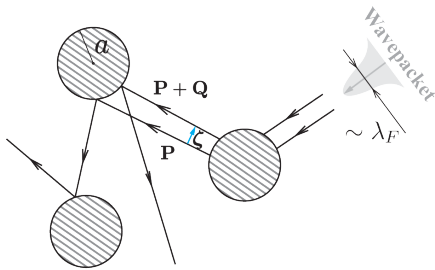


FIG. 1. (Colour online) Classical trajectories of electrons scattered by impurities.

parallel momenta and slightly different impact parameters collide with an impurity, their momenta get scattered at slightly different angles, as shown in Fig. 1. During subsequent collisions and propagation between impurities, the distance and the angle between the trajectories grow further. This leads to the exponential divergence between trajectories, as was first found in Ref. [2] and as also confirmed by the calculations in this paper, so long as the distance between trajectories remains smaller than the characteristic impurity size a . As soon as the distance between the trajectories exceeds the impurity size, the classical motion of electrons becomes uncorrelated and the OTOC ceases to grow exponentially.

The typical initial distance between the trajectories which contribute to the OTOC is determined by functions $K^{\alpha\beta}$, Eq. (3), at $t = 0$ and, thus, by the function g , Eq. (6), whose width may be estimated as $\lambda_F = 2\pi/p_F$ for momenta \mathbf{p}_1 and \mathbf{p}_2 near the Fermi surface. As a result of impurity collisions, the functions $K^{\alpha\beta}$ gets broadened to the characteristic width a in time on the order of the Ehrenfest time $t_E = \lambda^{-1} \ln(p_F a)$.

When considering the OTOC evolution on distances $|\mathbf{R}_1 - \mathbf{R}_2| \gg \lambda_F$, it is possible to make the approximation $g(\mathbf{R}_1 - \mathbf{R}_2, \mathbf{p}_1, \mathbf{p}_2) \approx -(2\pi)^d \delta(\mathbf{p}_1 - \mathbf{p}_2) \delta(\mathbf{R}_1 - \mathbf{R}_2) f_{\mathbf{p}_1} (1 - f_{\mathbf{p}_1})$. It follows then from Eq. (5) that

$$\left\langle [\hat{P}_z(t), \hat{P}_z(0)]^2 \right\rangle = \left\langle \left(\frac{\partial p_z(t)}{\partial z(0)} \right)^2 \right\rangle_{g, \text{dis}}, \quad (7)$$

where $p_z(t)$ is the momentum of an electron along a classical trajectory with given initial conditions (\mathbf{p}, \mathbf{r}) ; $z(0)$ is the coordinate along the z -axis at $t = 0$; and the averaging on the right-hand side is carried out with respect to the impurity locations (dis) and the initial momentum \mathbf{p} and coordinate \mathbf{r} of a classically moving electron:

$$\langle \dots \rangle_g = - \int_{\mathbf{p}, \mathbf{r}} \dots f_{\mathbf{p}} (1 - f_{\mathbf{p}}). \quad (8)$$

Eqs. (7) and (8) illustrate that the momentum-OTOC characterises the sensitivity of electron momenta at time t to the change of the initial coordinates.

To obtain the momentum divergence of the classical electron trajectories we introduce the separation ζ between respective pieces of the trajectories, as shown in Fig. 1. Such a separation vector is well-defined, so long as the trajectories are close; the respective pieces between two consecutive collisions may then be considered almost parallel. By analysing the scattering on a single impurity and free propagation between the impurities, we derive (the details will be reported elsewhere [28]) the equations for the evolution of the average separation ζ , the momentum difference \mathbf{Q} between the electrons (see Fig. 1) and the correlator $\langle \mathbf{Q} \cdot \zeta \rangle$ between the momentum difference \mathbf{Q} and vector ζ :

$$\begin{cases} \frac{d}{dt} \langle Q^2 \rangle = \frac{4p_F^2 \lambda^3}{v_F^2} \langle \zeta^2 \rangle, \\ \frac{d}{dt} \langle \zeta^2 \rangle = \frac{2v_F}{p_F} \langle \zeta \cdot \mathbf{Q} \rangle, \\ \frac{d}{dt} \langle \zeta \cdot \mathbf{Q} \rangle = \frac{v_F}{p_F} \langle Q^2 \rangle, \end{cases} \quad (9)$$

where the averaging $\langle \dots \rangle$ is carried out with respect to the impurity locations; we assumed that the electron momenta are close to the Fermi momentum p_F and have velocities v_F ;

$$\lambda = \left(\frac{n_{\text{imp}} v_F^3}{4(d-1)} \int \left[\left(\frac{d\phi}{d\rho} \right)^2 + (d-2) \frac{\sin^2 \phi}{\rho^2} \right] S_{d-1} \rho^{d-2} d\rho \right)^{\frac{1}{3}} \quad (10)$$

is the classical Lyapunov exponent (for $d = 3$, the same leading rate of exponential divergence between trajectory pairs was reported in Ref. [2]); n_{imp} is the impurity concentration; $\phi(\rho)$ is the angle of scattering on a single impurity as a function of the impact parameter ρ , and S_{d-1} is the area of a unit sphere in a $d-1$ -dimensional space (in this paper we consider $d > 1$). According to Eqs. (9), the average momentum difference $\mathbf{Q}(t)$ between two trajectories with the same initial momentum p_F and separation ζ_0 is given by

$$\langle Q^2(t) \rangle = \frac{2}{3} \left(\frac{p_F \lambda \zeta_0}{v_F} \right)^2 \left[e^{2\lambda t} + 2e^{-\lambda t} \cos \left(\lambda t \sqrt{3} - \frac{2\pi}{3} \right) \right]. \quad (11)$$

OTOC in a non-interacting system. For sufficiently long times, exceeding the transport scattering time $\tau_{\text{tr}} = \{v_F n_{\text{imp}} \int S_{d-1} \rho^{d-2} [1 - \cos \phi(\rho)] d\rho\}^{-1}$, the quasiparticle momentum $\mathbf{p}(t)$ is uncorrelated with its initial direction, however, there are still correlations between close pairs of trajectories which contribute to the OTOC growth. Using Eqs. (7), (8) and (11), we find the OTOC growth in a weakly disordered non-interacting system:

$$F(t) = - \frac{2(d-1) p_F^2 \lambda^2 v_F}{3d^2 v_F^2} V \cdot T e^{2\lambda t}, \quad (12)$$

where we kept only the leading exponentially growing contribution; ν_F is the density of states at the Fermi surface in the d -dimensional conductor under consideration;

V is the volume of the system; and we assume that the temperature T is sufficiently high, $T \gg \lambda$. For very low temperatures, $T \ll \lambda$, the OTOC is given by Eq. (12) with T replaced by a constant of order λ .

Electrons far from the Fermi surface. So far we considered quasiparticles near the Fermi surface. We note, however, that quasiparticles far from the Fermi surface may yield significant contributions to the OTOC in a non-interacting system. Although their concentration is exponentially suppressed, $\propto e^{-|E-E_F|/T}$, their contribution to the OTOC grows exponentially with velocity, $\propto e^{\text{const}\cdot vt}$. Strictly speaking, the OTOC in a non-interacting system is dominated by the quasiparticles with the largest velocity in the band. However, in the presence of interaction, the inelastic relaxation rate grows rapidly away from the Fermi surface, $1/\tau(E) \propto |E - E_F|^2$ for $|E - E_F| \gg T$, which strongly suppresses the lifetime of excitations with high energies and their contributions to the OTOC. In this paper we, therefore, neglect such high-energy excitations and focus on the quasiparticles near the Fermi surface.

Effect of interaction on OTOCs. To the lowest order in the interaction strength [28], we derive the evolution of the correlation functions $K^{\alpha\beta}$, Eq. (3), between impurity collisions for small $\mathbf{p}_1 - \mathbf{p}_2$ in the form

$$\begin{aligned} \partial_t K^{\alpha\beta}(\mathbf{p}_1, \mathbf{p}_2) = & - \left(\frac{1}{\tau_\alpha(\mathbf{p}_1)} + \frac{1}{\tau_\beta(\mathbf{p}_2)} \right) K^{\alpha\beta}(\mathbf{p}_1, \mathbf{p}_2) \\ & + \frac{1}{\tau_\alpha(\mathbf{p}_1)} K^{\bar{\alpha}\beta}(\mathbf{p}_1, \mathbf{p}_2) + \frac{1}{\tau_\beta(\mathbf{p}_2)} K^{\alpha\bar{\beta}}(\mathbf{p}_1, \mathbf{p}_2), \end{aligned} \quad (13)$$

where we omitted the coordinate arguments of the functions $K^{\alpha\beta}$; the indices α and β again label electrons and holes ($\alpha, \beta = e, h$) and we have introduced the electron scattering rate

$$\begin{aligned} \frac{1}{\tau_e(\mathbf{p})} = & 2\pi \int_{\mathbf{p}', \mathbf{q}} (1 - f_{\mathbf{p}'}) (1 - f_{\mathbf{p}+\mathbf{q}}) f_{\mathbf{p}'+\mathbf{q}} |w(\mathbf{q})|^2 \\ & \delta(\xi_{\mathbf{p}} + \xi_{\mathbf{p}'+\mathbf{q}} - \xi_{\mathbf{p}+\mathbf{q}} - \xi_{\mathbf{p}'}) \end{aligned} \quad (14)$$

and a similar hole scattering rate given by Eq. (14) with the replacements $f \rightarrow 1 - f$. For excitations on the Fermi surface and for short-range interactions under consideration, $1/\tau_e = 1/\tau_h = 1/\tau(T) = T^2 \cdot C k_F^{2d-3} [\int_{\mathbf{r}} |w(\mathbf{r})|^2] / v_F^3$, where the constant $C \sim 1$ depends on the space dimensionality and the details of the Fermi surface.

Equation (13) may be understood qualitatively as follows. When two quasiparticles α and β propagate along close trajectories with close momenta \mathbf{p}_1 and \mathbf{p}_2 , each of them may get inelastically scattered, with rates $1/\tau_\alpha$ and $1/\tau_\beta$, as reflected by the first term on the right-hand side of Eq. (13). In the spirit of Ref. [27], quasiparticle states with significantly different momenta may be considered as an external bath. If one electron in a pair gets

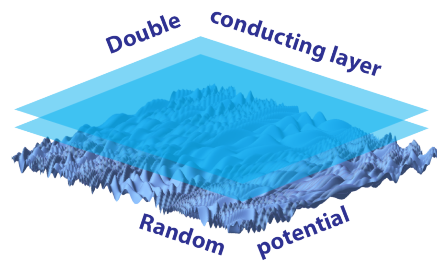


FIG. 2. (Colour online) Setup for measuring OTOCs; two layers of particles exposed to the same random potential.

scattered, its momentum changes significantly due to the short-range nature of the interaction, further motion of these electrons is uncorrelated, and they no longer contribute to the exponential growth of the OTOC. There are also reverse processes, described by the last two terms in Eq. (13); a pair of electrons with close momenta may be created by inelastic processes; the respective contributions to K^{ee} , for example, require the existence of holes with momenta under consideration and are thus proportional to $K^{eh,he}$. We note also that we assume short-range interactions, with radius $r_0 \ll |\mathbf{R}_1 - \mathbf{R}_2|$, which do not lead to direct interaction between electrons on close trajectories. Depending on whether or not the interaction radius r_0 is smaller than λ_F , Eqs. (13) apply to the entire OTOC evolution or to its later stages; in the latter case one has to use other effective initial conditions in place of (5).

Eqs. (13) describe the evolution of the correlation functions $K^{\alpha\beta}$ between impurity collisions and indicate that distributions with $K^{\alpha\alpha} \propto -K^{\alpha\bar{\alpha}}$ for all α , as corresponds to the initial conditions (5), relax with the rate $1/\tau_e + 1/\tau_h = 2/\tau(T)$, where we have taken into account that electrons and holes have equal relaxation rates $1/\tau(T)$ on the Fermi surface. Thus, inelastic scattering suppresses correlations between pairs of electrons with close momenta and leads to the exponential suppression of the OTOC as described by the second term in the exponent in Eq. (1). At large temperatures or interaction strengths, this suppression prevents exponential growth, and a chaotic system becomes non-chaotic.

Relation to level statistics. Usually, systems which exhibit chaotic dynamics in the classical limit also display Wigner-Dyson statistics of the energy levels [1]. We conjecture that the transition between chaotic and non-chaotic behaviour, discussed in this paper, may also be accompanied by the change of energy-level statistics characterised by the correlator $R_2(\omega) = \langle \rho(E - \frac{\omega}{2}) \rho(E + \frac{\omega}{2}) \rangle$, where $\rho(E) = -\frac{1}{\pi V} \text{Im} \int_{\mathbf{r}} G^R(\mathbf{r}, \mathbf{r}, E)$ is the quasiparticle density of states, and the averaging is carried out with respect to the impurity locations. We leave, however, a rigorous analysis of the relation between the exponential growth of OTOCs and energy level statistics for future studies.

Potential for experimental observation in double layers. The evolution of the correlators $K^{\alpha\beta}$ is similar to that of the correlations between two layers of particles exposed to the same random potential, as shown in Fig. 2, which suggests a way for experimental observations of the OTOC and the transition between chaotic and non-chaotic behaviour by observing momentum correlations between the two layers of, e.g., ultracold atoms or molecules. Indeed, as it has been demonstrated in Ref. [27], the OTOCs in a system coupled to a classical environment may be mapped onto the evolution of two copies of that system coupled to the same environment. Initial correlations between the particles in the layers may be induced, for example, by switching on attractive interactions between the layers for a short time.

Conclusion. We have demonstrated that a weakly disordered metal with short-range interactions displays a transition between quantum-chaotic and non-chaotic dynamics, identified through the OTOC behaviour, when changing the temperature or interaction strength. We conjecture that the transition is accompanied by a change in the level statistics of the system. Natural other future research directions include analysing other models of interaction, quasiparticle dispersion, interplay with weak-localisation effects, etc. Also, we expect our results to hold qualitatively if the inelastic scattering comes from phonons or other types of external baths instead of electron-electron interactions, because such a bath may suppress correlations between electron trajectories similarly to interactions.

Another question, which deserves a separate investigation, is the effect of rare events on the quantum chaotic dynamics. Exponentially-rare fluctuations of the impurity density in a disordered material may lead to sparse regions with large values of the Lyapunov exponent, which may affect the exponential growth of OTOCs on sufficiently short times scales. A detailed analysis of the effect of such rare events on the transition discussed in this paper and on other aspects of quantum chaos will be presented elsewhere.

We acknowledge useful discussions with J. Maldacena and B. Swingle. Our research was supported financially by NSF-DMR 1613029, US-ARO contract No. W911NF1310172 (SVS) and U.S. Department of Energy BES-DESC0001911 and Simons Foundation (VMG). AVG and SVS were supported by NSF QIS, AFOSR, NSF PFC at JQI, ARO MURI, ARO and ARL CDQI.

-
- [1] K. B. Efetov, *Supersymmetry in Disorder and Chaos* (Cambridge University Press, New York, 1999).
 [2] A. Larkin and Y. N. Ovchinnikov, “Quasiclassical method in the theory of superconductivity,” *Sov. Phys. JETP* **28**, 960 (1969).

- [3] J. Maldacena, S. H. Shenker, and D. Stanford, “A bound on chaos,” *JHEP* **8**, 106 (2016).
 [4] Igor L. Aleiner, Lara Faoro, and Lev B. Ioffe, “Microscopic model of quantum butterfly effect: out-of-time-order correlators and traveling combustion waves,” (2016), arXiv:1609.01251.
 [5] R. Fan, P. Zhang, H. Shen, and H. Zhai, “Out-of-Time-Order Correlation for Many-Body Localization,” *Science Bull.* **62**, 707 (2017).
 [6] Y. Chen, “Universal logarithmic scrambling in many body localization,” *ArXiv e-prints* (2016), arXiv:1608.02765 [cond-mat.dis-nn].
 [7] B. Swingle and D. Chowdhury, “Slow scrambling in disordered quantum systems,” *Phys. Rev. B* **95**, 060201 (2017).
 [8] Y. Huang, Y.-L. Zhang, and X. Chen, “Out-of-time-ordered correlators in many-body localized systems,” *Ann. Phys.* **529**, 1600318 (2017).
 [9] Efim B. Rozenbaum, Sriram Ganeshan, and Victor Galitski, “Lyapunov exponent and out-of-time-ordered correlator’s growth rate in a chaotic system,” *Phys. Rev. Lett.* **118**, 086801 (2017).
 [10] Aavishkar A. Patel, Debanjan Chowdhury, Subir Sachdev, and Brian Swingle, “Quantum butterfly effect in weakly interacting diffusive metals,” *Phys. Rev. X* **7**, 031047 (2017).
 [11] D. Bagrets, A. Altland, and A. Kamenev, “Power-law out of time order correlation functions in the SYK model,” *Nuclear Physics B* **921**, 727–752 (2017).
 [12] Y. Werman, S. A. Kivelson, and E. Berg, “Quantum chaos in an electron-phonon bad metal,” *ArXiv e-prints* (2017), arXiv:1705.07895 [cond-mat.str-el].
 [13] N. Y. Yao, F. Grusdt, B. Swingle, M. D. Lukin, D. M. Stamper-Kurn, J. E. Moore, and E. A. Demler, “Interferometric Approach to Probing Fast Scrambling,” *ArXiv e-prints* (2016), arXiv:1607.01801.
 [14] A. Bohrdt, C. B. Mendl, M. Endres, and M. Knap, “Scrambling and thermalization in a diffusive quantum many-body system,” *New J. Phys.* **19**, 063001 (2017).
 [15] B. Swingle, G. Bentsen, M. Schleier-Smith, and P. Hayden, “Measuring the scrambling of quantum information,” *Phys. Rev. A* **94**, 040302 (2016).
 [16] Guanyu Zhu, Mohammad Hafezi, and Tarun Grover, “Measurement of many-body chaos using a quantum clock,” *Phys. Rev. A* **94**, 062329 (2016).
 [17] I. Danshita, M. Hanada, and M. Tezuka, “Creating and probing the Sachdev-Ye-Kitaev model with ultracold gases: Towards experimental studies of quantum gravity,” *Prog. Theor. Exp. Phys.* **2017**, 083101 (2017).
 [18] M. Gärttner, J. G. Bohnet, A. Safavi-Naini, M. L. Wall, J. J. Bollinger, and A. M. Rey, “Measuring out-of-time-order correlations and multiple quantum spectra in a trapped ion quantum magnet,” *ArXiv e-prints* (2016), arXiv:1608.08938.
 [19] Naoto Tsuji, Philipp Werner, and Masahito Ueda, “Exact out-of-time-ordered correlation functions for an interacting lattice fermion model,” *Phys. Rev. A* **95**, 011601 (2017).
 [20] Jun Li, Ruihua Fan, Hengyan Wang, Bingtian Ye, Bei Zeng, Hui Zhai, Xinhua Peng, and Jiangfeng Du, “Measuring out-of-time-order correlators on a nuclear magnetic resonance quantum simulator,” *Phys. Rev. X* **7**, 031011 (2017).
 [21] N. Yunger Halpern, B. Swingle, and J. Dressel, “The

- quasiprobability behind the out-of-time-ordered correlator,” ArXiv e-prints (2017), arXiv:1704.01971.
- [22] Nicole Yunger Halpern, “Jarzynski-like equality for the out-of-time-ordered correlator,” *Phys. Rev. A* **95**, 012120 (2017).
- [23] D. M. Basko, I. L. Aleiner, and B. L. Altshuler, “Metal insulator transition in a weakly interacting many-electron system with localized single-particle states,” *Ann. Phys.* **321**, 1126 (2006).
- [24] See Ref. [29] for review.
- [25] A. A. Abrikosov, L. P. Gorkov, and I. E. Dzyaloshinski, *Methods of Quantum Field Theory in Statistical Physics* (Dover, New York, 1975).
- [26] A. Kamenev, *Field Theory of Non-Equilibrium Systems* (Cambridge Univ. Press, Cambridge, 2011).
- [27] S. V. Syzranov, A. V. Gorshkov, and V. Galitski, “Out-of-time-order correlators in finite open systems,” (2017), arXiv:1704.08442.
- [28] S. V. Syzranov, A. V. Gorshkov, and V. Galitski, (2017), coming soon.
- [29] R. Nandkishore and D. A. Huse, “Many-Body Localization and Thermalization in Quantum Statistical Mechanics,” *Annual Review of Condensed Matter Physics* **6**, 15–38 (2015).